Supporting information

Atomically dispersed Ru doped in IrO_x nano clusters for the enhanced oxygen evolution reaction in acidic media

Yan Dong, [1,2,3] Yanle Li, [1,5] Yichao Lin,*[1,2] Anyang Chen,[1] Mengting Deng,[1] Linjuan Zhang,[4] Ziqi Tian,*[1,2] and Liang Chen*[1,2]

1. Key Laboratory of Advanced Fuel Cells and Electrolyzers Technology of Zhejiang Province, Ningbo Institute of Materials Technology and Engineering, Chinese Academy of Sciences, Ningbo, Zhejiang 315201, P.R. China
2. University of Chinese Academy of Sciences, Beijing 100049, P.R. China
3. School of Materials Science and Engineering, Hainan University, Haikou 570228, P. R. China
4. Key Laboratory of Interfacial Physics and Technology, Shanghai Institute of Applied Physics, Chinese Academy of Sciences, Shanghai 201800, P. R. China
5. Yangtze Delta Region Institute (Huzhou), University of Electronic Science and Technology of China, Huzhou, Zhejiang 313000, P. R. China

E-mail: yclin@nimte.ac.cn, tianziqi@nimte.ac.cn, chenliang@nimte.ac.cn

EXPERIMENTAL METHODS

Chemicals. All chemicals were analytical grade and used without further purification. Ruthenium chloride hydrate ($RuCl_3 \cdot xH_2O$), Iridium chloride hydrate ($IrCl_3 \cdot xH_2O$), formic acid (99%) and 1-Methyl-2-pyrrolidinone (NMP) were purchased from Aladdin Chemical Reagent limited corporation. Carbon paste was purchased from BAS incorporate. The deionized (DI) water used throughout all experiments was purified through a Millipore system.

Synthesis of Ir clusters. $IrCl_3 \cdot xH_2O$ (30 mg) was dispersed in 5 mL formic acid. Then, the above solution was mixed with 15 mL NMP. After agitated stirring for 30 min, the mixed solution was transferred into 50 mL Teflon stainless steel and heated at 100 °C for 5 h. After that, the black precipitated was collected and washed three times with ethanol, and dried in an oven at 60 °C overnight.

Synthesis of Ru-IrO_x clusters. $IrCl_3 \cdot xH_2O$ (30 mg) and $RuCl_3 \cdot xH_2O$ (30 mg) were dispersed in 5 mL formic acid. Then, the above solution was mixed with 15 mL NMP. After agitated stirring for 30 min, the mixed solution was transferred into 50 mL Teflon stainless steel and heated at 100 °C for 5 h. After that, the black precipitated was collected and washed three times with ethanol, and dried in an oven at 60 °C overnight.

Electrocatalytic OER measurements. In a typical procedure, 4 mg of Ru-IrO_x clusters and 4 mg carbon paste were mixed and grinded for 20 min. Then, the mixtures were added to 1 ml of water/ethanol (3:1, v/v) containing 15 μL Nafion solution (5 %, Sigma-Aldrich). After the mixtures were sonicated for 30 min, 200 μL catalyst ink was dipped on a carbon paper (1x1 cm) and dried at room temperature. A three-electrode set-up was used for electrocatalytic OER measurements. A platinum mesh was used as the counter electrode, while a saturated Hg/Hg_2SO_4 electrode after calibrated in H_2-saturated 0.5 M H_2SO_4 solution was used as reference electrode. The potential difference between the Hg/Hg_2SO_4 reference electrode and reversible hydrogen electrode is 0.704 V (Fig. S9). All measurements were performed in 0.5 M H_2SO_4 solution at room temperature. Cyclic voltammograms (CVs) tests were collected at a scan rate of 50 mV/s typically between 1.004 and 1.504 V vs. RHE (Fig. S10). Linear

sweep voltammetry (LSV) curves were collected at a scan rate of 5 mV/s from 1.204 and 1.704 V. Chronopotentiometric measurements were carried out at applying constant current (10 mA cm^{-2}) for up to 150 h. Electrochemical impedance spectroscopy (EIS) were performed at 0.8 V.

PEM water electrolyzer. 16 mg of Ru-IrO_x clusters were dispersed to 4 ml of water/ethanol (3:1, v/v) containing 120 μL Nafion solution (5 %, Sigma-Aldrich). After the mixtures were sonicated for 30 min, the prepared catalyst ink was sprayed on a Nafion 117 membrane (2 x 2 cm) and dried at room temperature. The cathode side was coated with 1 mg cm^{-2} of commercial 20 wt % Pt/C (Sigma-Aldrich). Subsequently, MEA and two protected PTFE sheet were hot pressed together at 135 ^{o}C for 10 minutes with a pressure of 10 MPa. A carbon fiber paper (Toray H-090, 280 μm) and platinum plated titanium felt (250 μm) work as cathodic and anodic gas diffusion layer, respectively. The tightening force for the assembly of electrolytic cell is 6 N·m. The performance of the single cell was carried out at room temperature with DI water pumped into the anode side.

Computational Details. All the spin-polarized density functional theory (DFT) calculations were conducted using the Vienna Ab-initio Simulation Package (VASP) software.[1] The exchange-correlation interaction was described with generalized gradient approximation (GGA)-Revised Perdew-Burke-Ernzerhof (RPBE) functional.[2] The projected augmented-wave (PAW) method was employed to depict the interaction of ions and electrons.[3] The van der Waals interactions was considered with the DFT-D3 method.[4] The cutoff energy for the plane-wave-basis set was set as 400 eV. The convergence criteria for energy of electronic self-consistence loops and force of ionic relaxation loops were set as 10^{-4} eV and 0.03 eV/Å, respectively. As shown in Fig. S22a, the IrO_2 and RuO_2 slab models are constructed by their (3 × 2) (110) surfaces, which are the most stable rutile-type surfaces[5]. The slab included 12 atomic layers and a 15 Å vacuum layer in the perpendicular direction of the (110) surface to avoid the interaction between adjacent images. The Ru doped IrO_2 is constructed by replacing one coordinately unsaturated Ir atom on the IrO_2(110) surface,

as exhibited in Fig. S22. The top six atomic layers and adsorbed species were allowed to relax and other atoms were fixed during the geometrical optimization. The k-points to sample the Brillouin zone were set as 3 × 2 × 1 for optimization and Bader charge analysis, and 6 × 4 × 1 for density of states (DOS) calculations.

The four-electron process was adopted to investigate the oxygen evolution reaction (OER) mechanism, including the following four elementary steps.[5]:

$$H_2O + * \rightarrow *OH + H^+ + e^- \quad (1)$$

$$*OH \rightarrow *O + H^+ + e^- \quad (2)$$

$$H_2O + *O \rightarrow *OOH + H^+ + e^- \quad (3)$$

$$*OOH \rightarrow * + O_2 + H^+ + e^- \quad (4)$$

where asterisk (-*) represent an adsorption site on the surface, and a proton (H^+) and an electron (e^-) transfer took place at each step. The free energy change of each step was computed with the following equations:

$$\Delta G_1 = E(*OH) - E(*) - E_{H2O} + 1/2E_{H2} + (\Delta ZPE - T\Delta S)$$

$$\Delta G_2 = E(*O) - E(*OH) + 1/2E_{H2} + (\Delta ZPE - T\Delta S)$$

$$\Delta G_3 = E(*OOH) - E(*O) - E_{H2O} + 1/2E_{H2} + (\Delta ZPE - T\Delta S)$$

$$\Delta G_4 = E(*) - E(*OOH) + E_{O2} + 1/2E_{H2} + (\Delta ZPE - T\Delta S)$$

where E(*), E(*OH), E(*O) and E(*OOH) are the computed energies of the surface and the adsorbed *OH, *O and *OOH species, respectively. The zero point energy and the entropy included in $\Delta G_1 \sim \Delta G_4$ are taken from the reference.[6]

The surface Pourbaix diagram was constructed based on the following electrochemical steps on $IrO_2(110)$ surface:

$$OH@IrO_2(110) + H^+ + e^- = IrO_2(110) + H_2O, \quad (5)$$

$$O@IrO_2(110) + H^+ + e^- = OH@IrO_2(110). \quad (6)$$

The electromotive forces for equation (1) and (2) were calculated as $E = -\Delta G/n$, where ΔG was the free energy changes in eV, and n was the number of electrons transferred in the reaction. To obtain the surface Pourbaix diagram, the relation between applied potential, E, and pH was analyzed as:

$$E(OH@IrO_2(110)) = E^0(OH@IrO_2(110)/IrO_2(110)) - 0.059 * pH, \quad (7)$$

$$E(O@IrO_2(110)) = E^0(O@IrO_2(110)/OH@IrO_2(110)) - 0.059 * pH. \quad (8)$$

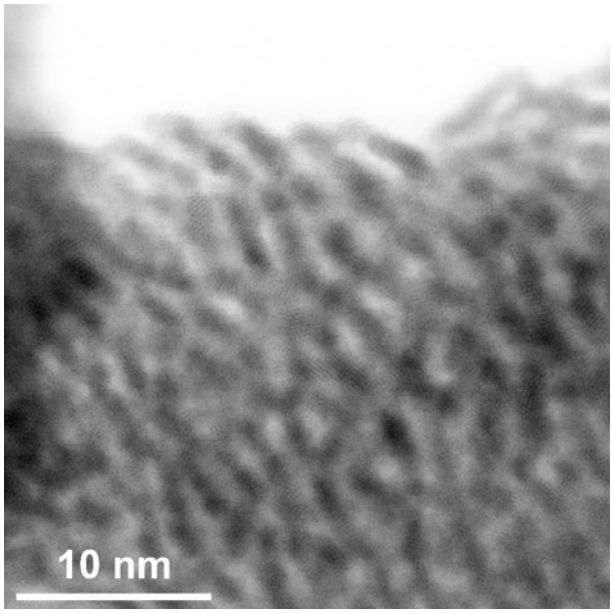

Fig. S1. HRTEM image of Ir clusters.

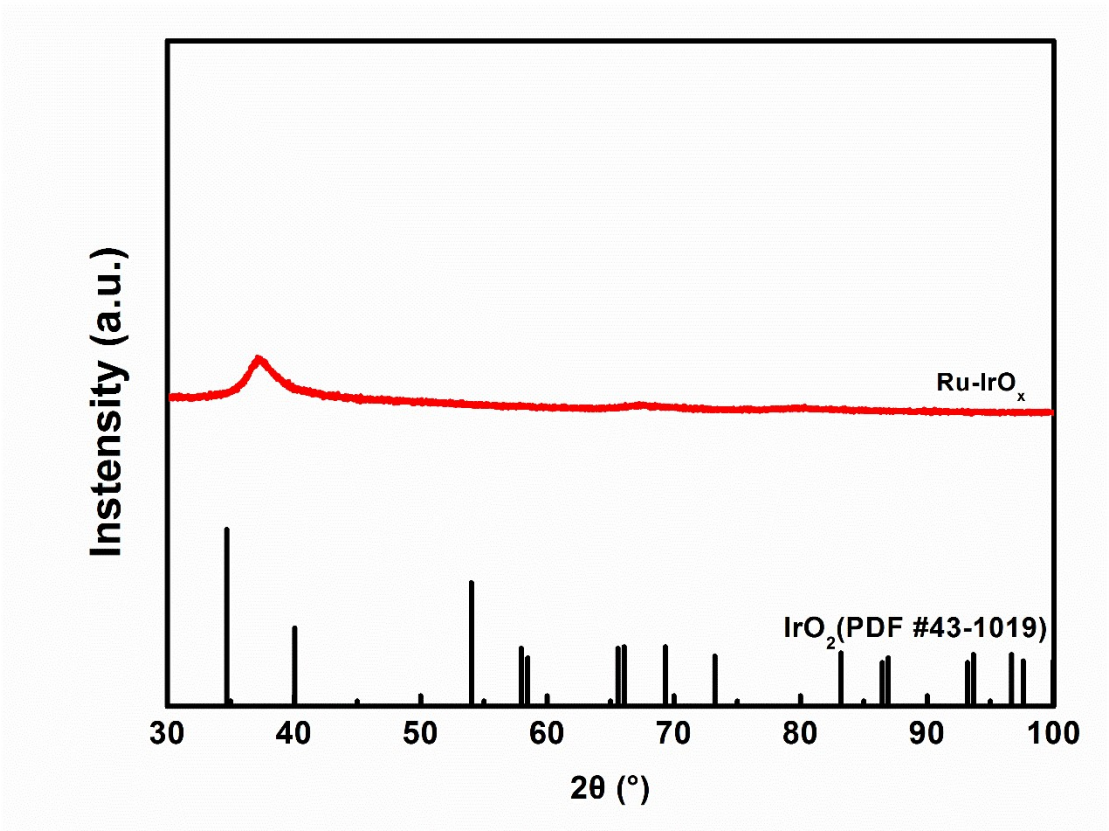

Fig. S2. XRD pattern of Ru-IrO_x.

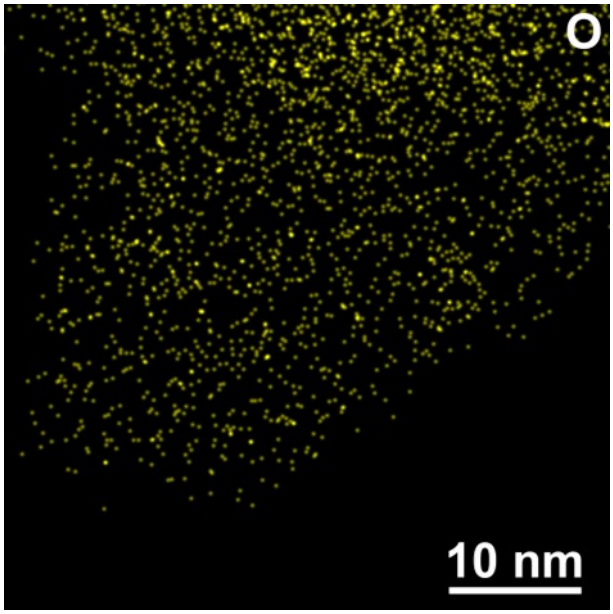

Fig. S3. HAADF-STEM image and corresponding EDS maps of O.

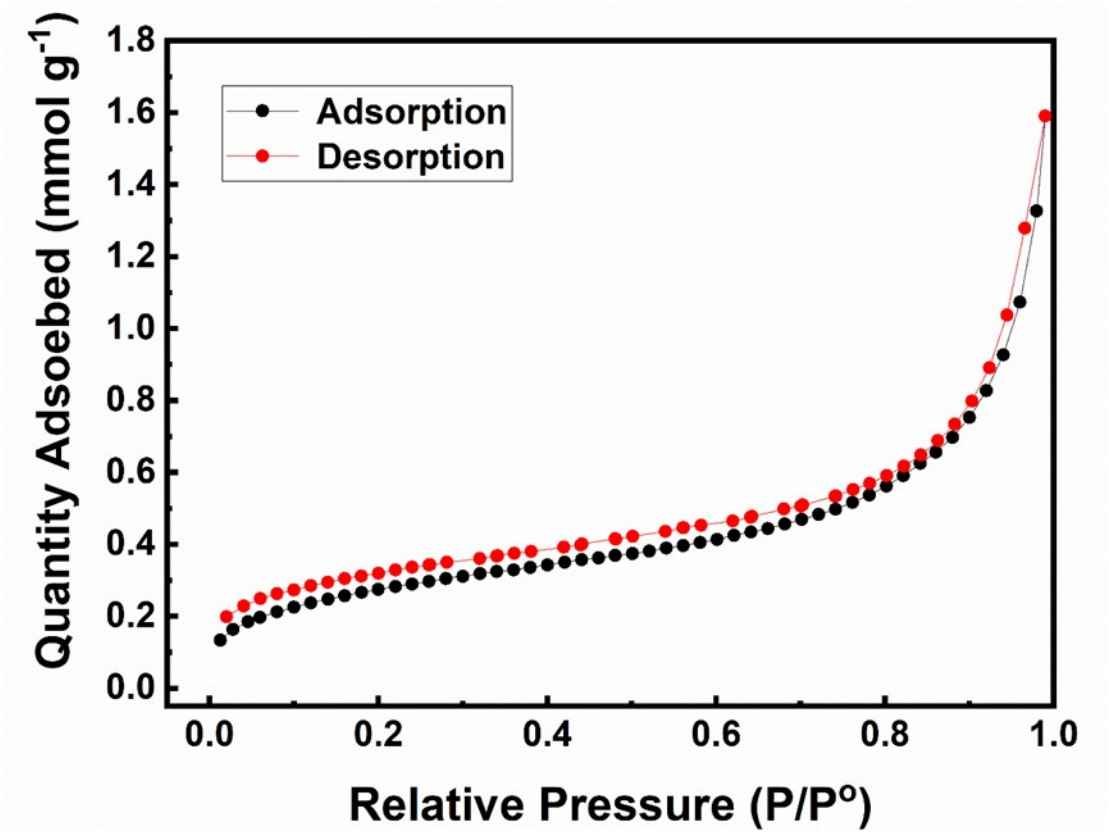

Fig. S4. N_2 adsorption-desorption isotherm of Ru-IrO_x clusters.

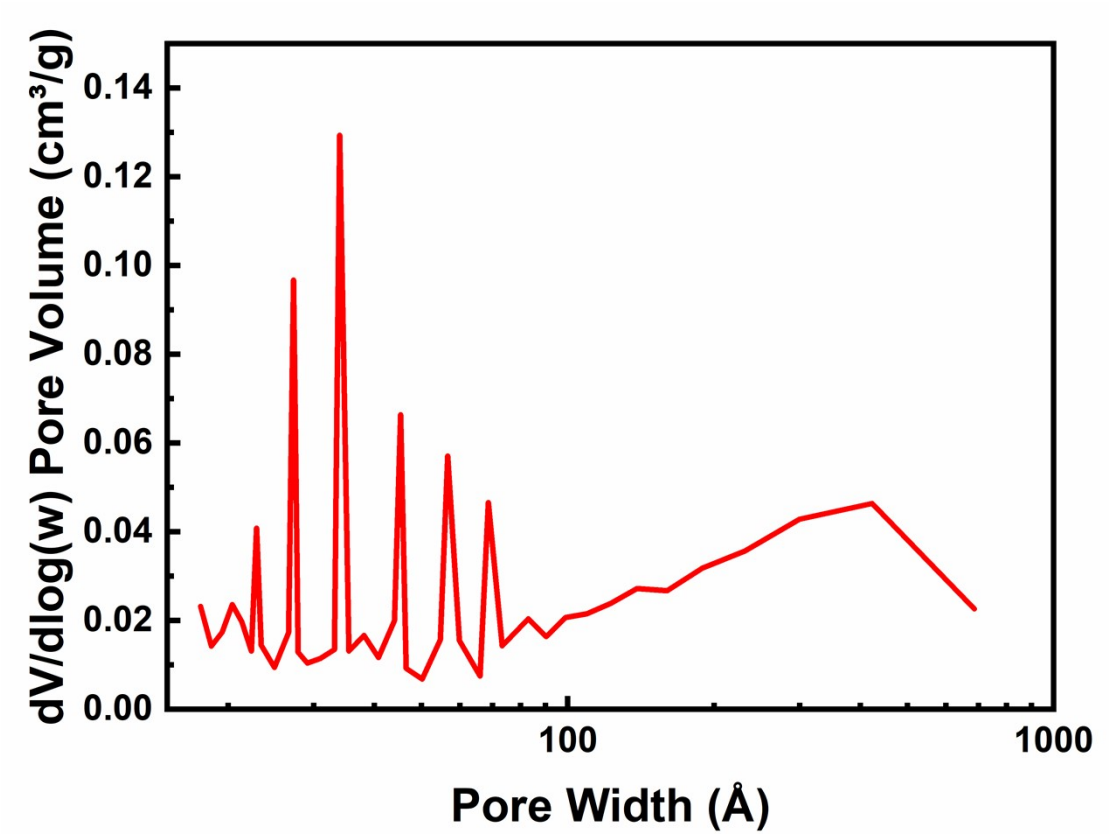

Fig. S5. The micropore size distribution plot of Ru-IrO_x clusters.

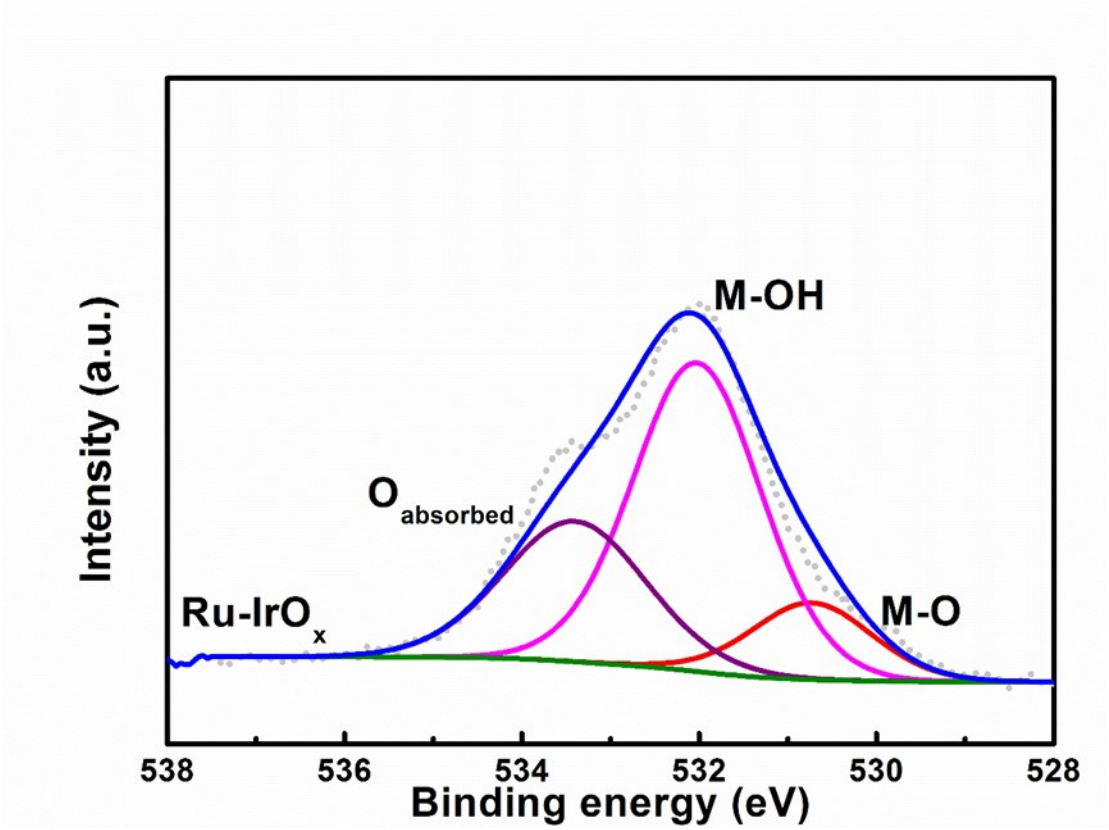

Fig. S6. XPS results of O 2p for Ru-IrO_x clusters.

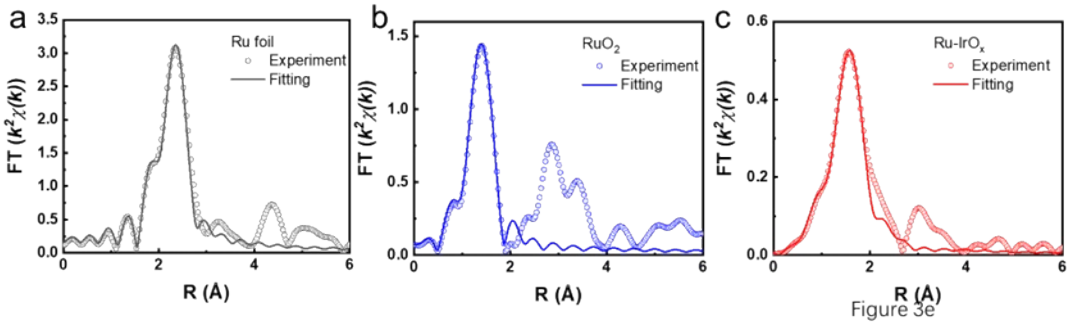

Fig. S7. EXAFS fitting curve for Ru K-edge of Ru foil. b) EXAFS fitting curve for Ru K-edge of RuO_2. c) EXAFS fitting curve for Ru K-edge of Ru-IrO_x.

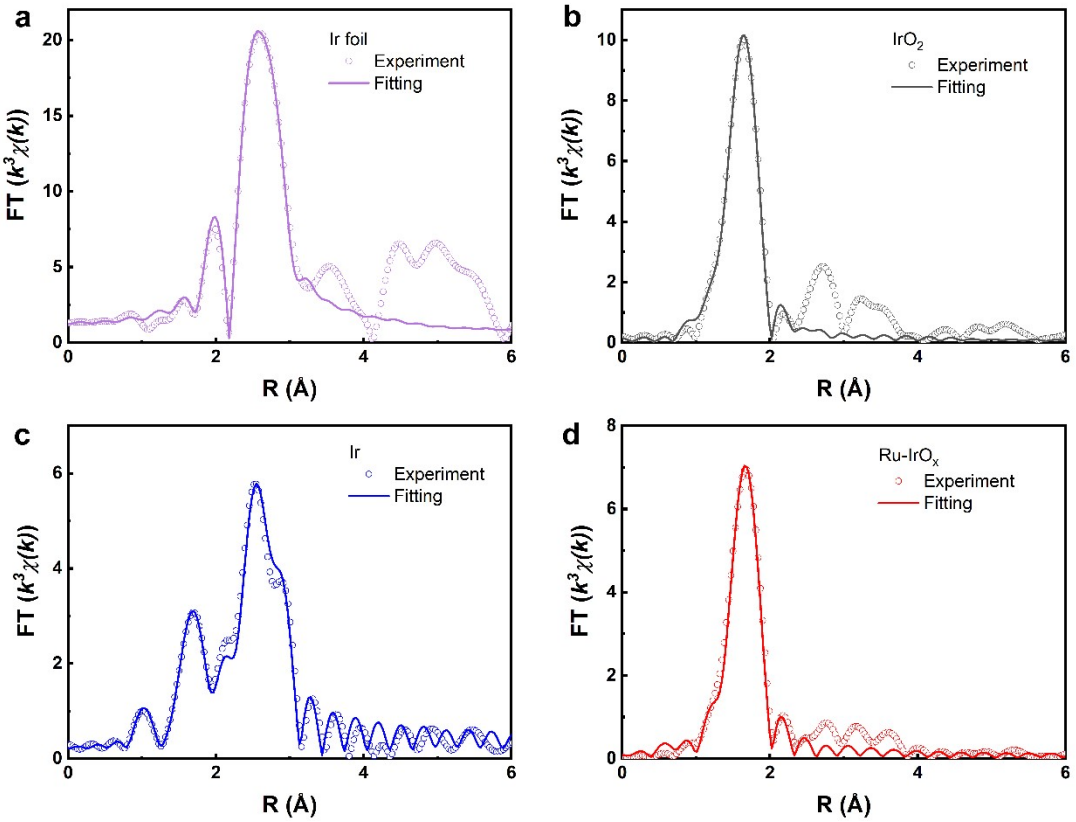

Fig. S8. a) EXAFS fitting curve for Ir L_3-edge of Ir foil. b) EXAFS fitting curve for Ir L_3-edge of IrO_2. c) EXAFS fitting curve for Ir L_3-edge of Ir clusters. d) EXAFS fitting curve for Ir L_3-edge of Ru-IrO_x clusters.

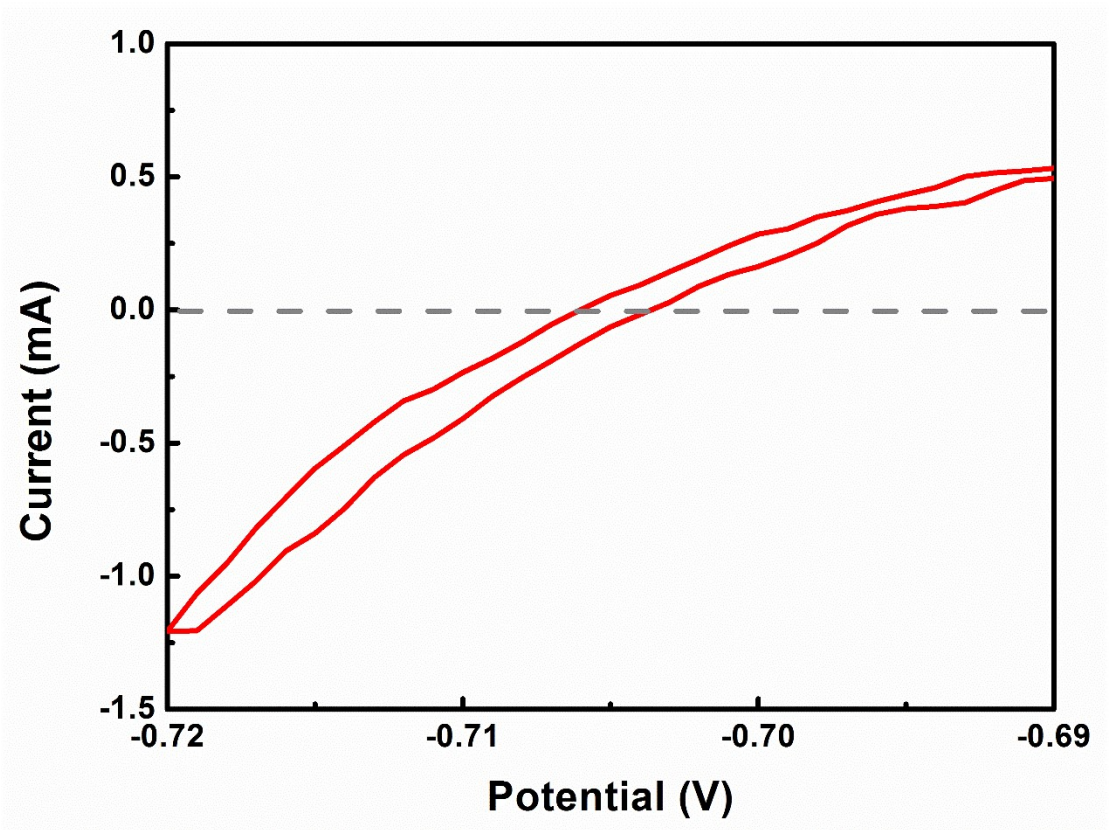

Fig. S9. Calibration of the $Hg/HgSO_4$ electrode (saturated potassium sulfate) in 0.5 M H_2SO_4 electrolyte.

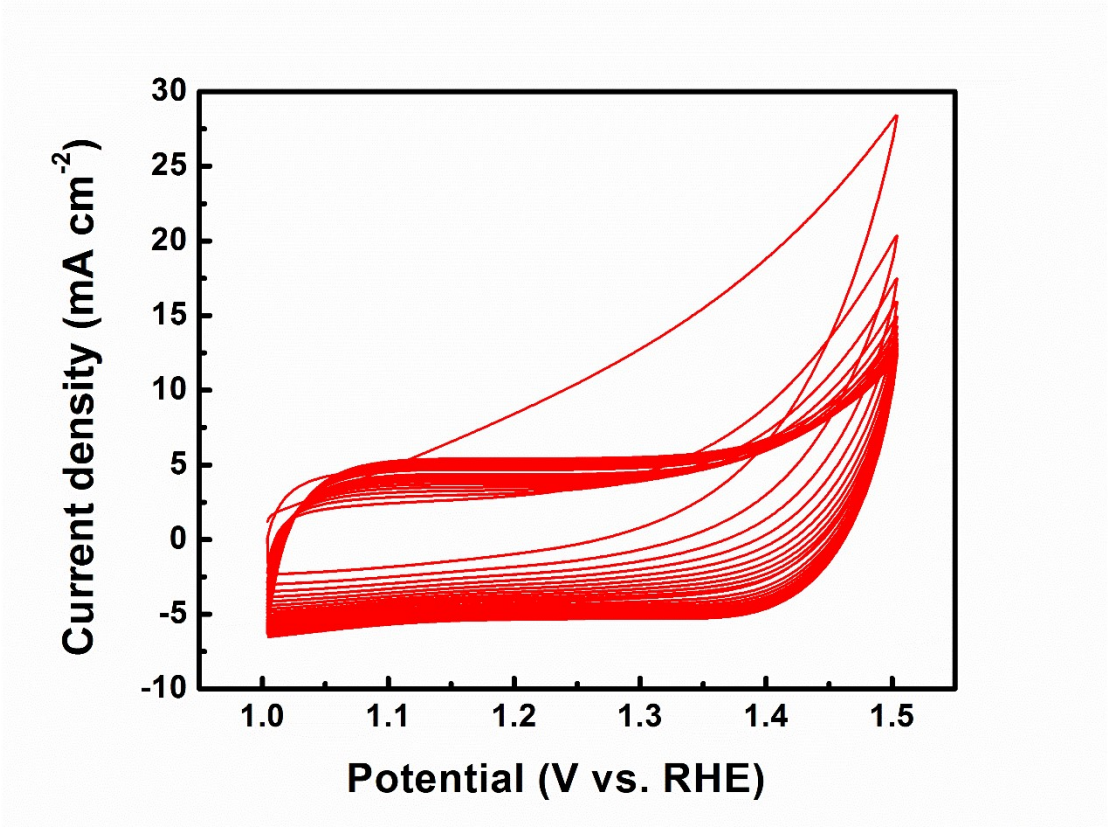

Fig. S10. CV curves of Ru-IrO_x clusters.

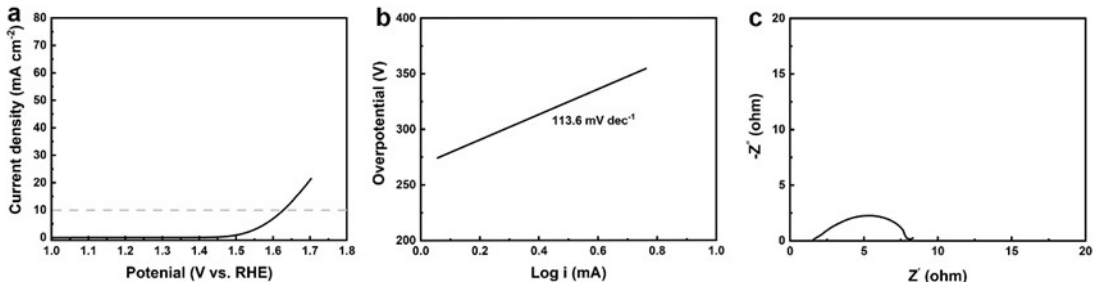

Fig. S11 a) LSV curves of commercial RuO2 for OER in 0.5 M H_2SO_4 solution. b) The corresponding Tafel plots of commercial RuO_2 for OER in 0.5 M H_2SO_4 solution. c) Nyquist plots of commercial RuO_2.

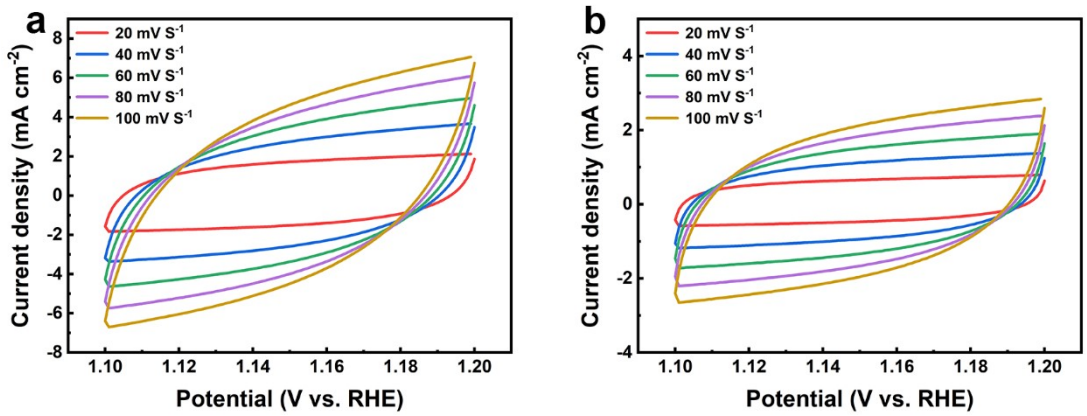

Fig. S12. a) CV curves of Ru-IrO_x measured in the range of 1.10 to 1.20 vs. RHE with the scam rate from 20 to 100 mV s^{-1}. b) CV curves of Ir measured in the range of 1.10 to 1.20 vs. RHE with the scam rate from 20 to 100 mV s^{-1}.

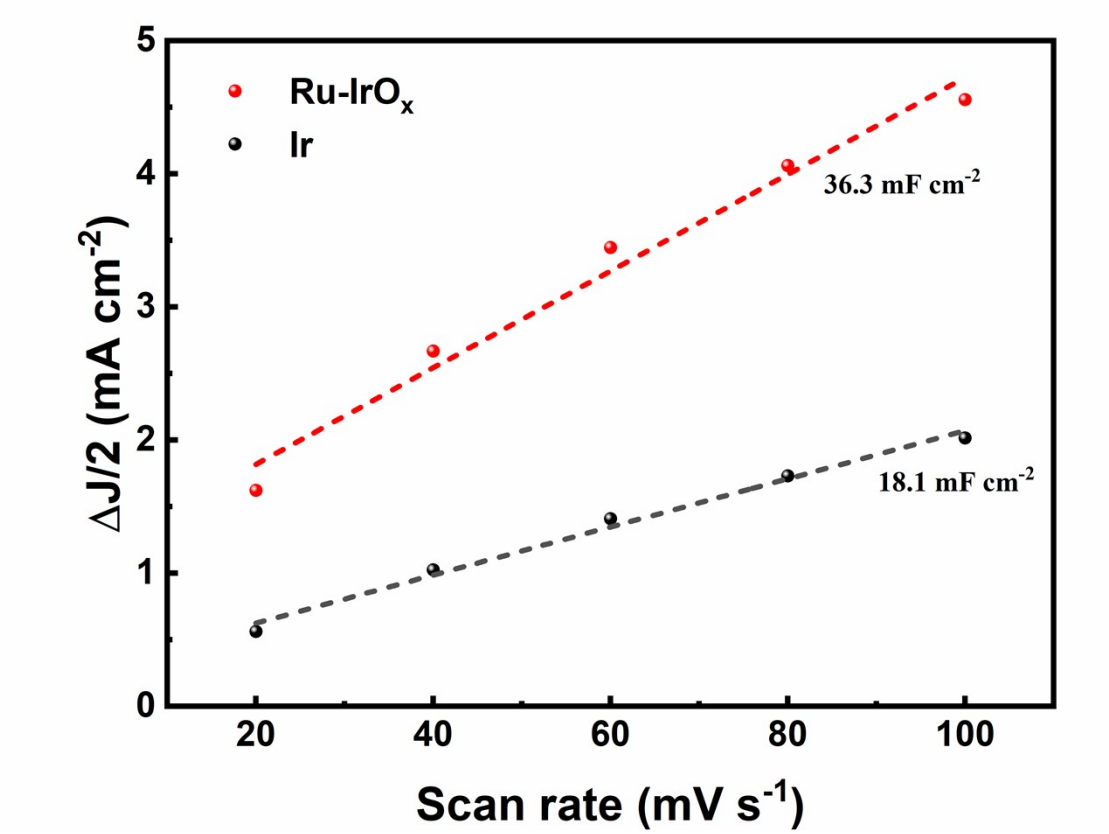

Fig. S13. Capacitive current against the scan rate and corresponding C_{dl} values estimated through linear fitting of the plots.

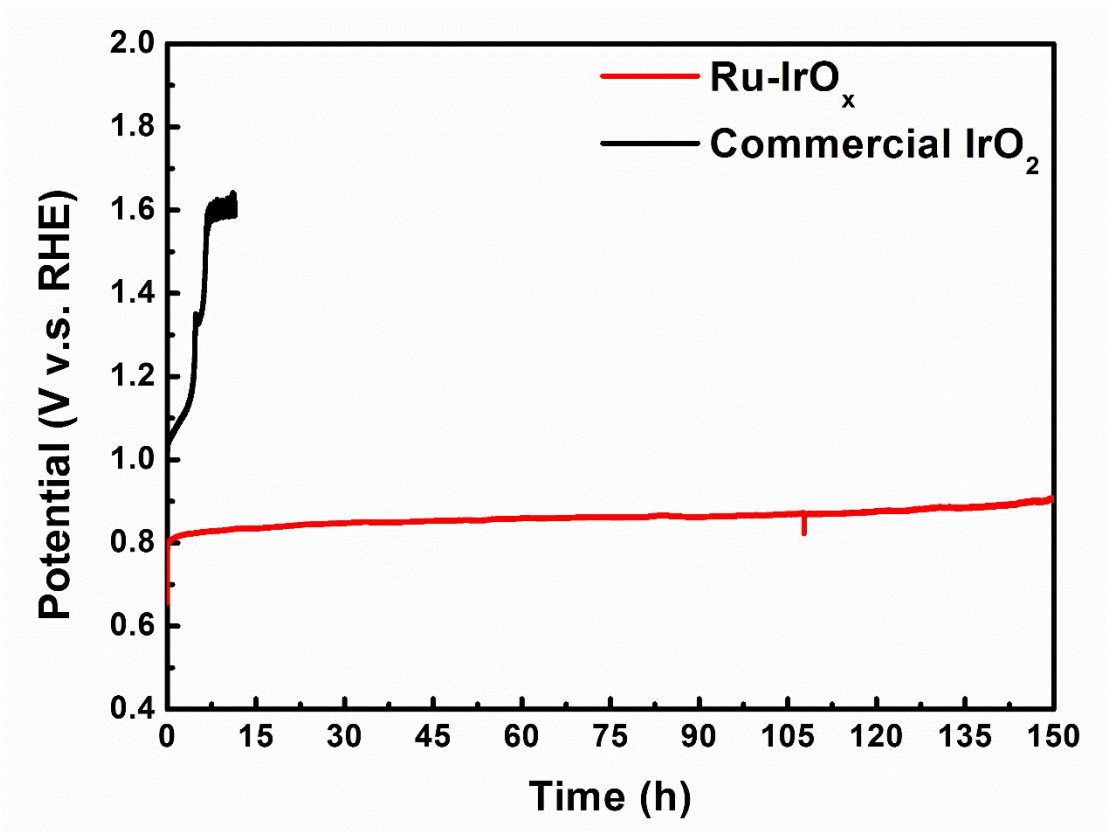

Fig. S14. Chronopotentiometric performance under constant current density of 10 mA cm^{-2} up to 150 h.

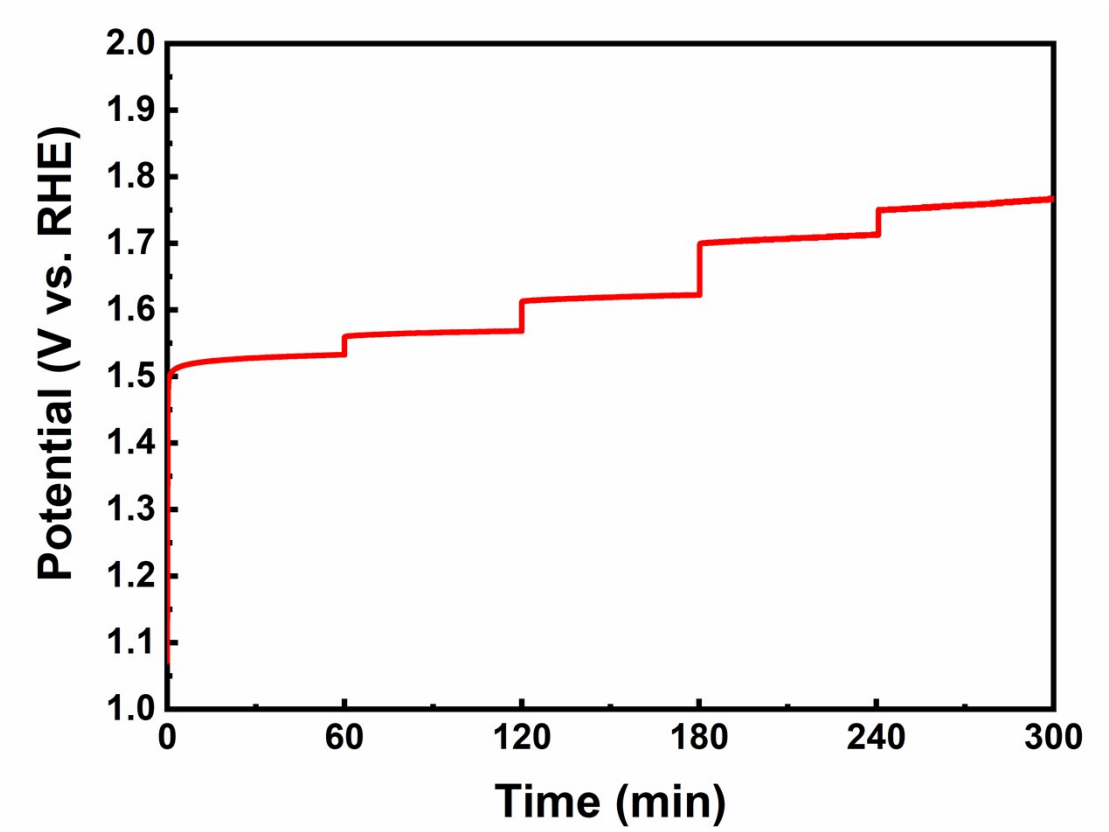

Fig. S15. Stable test at different current density from 10 to 100 mA cm^{-2}.

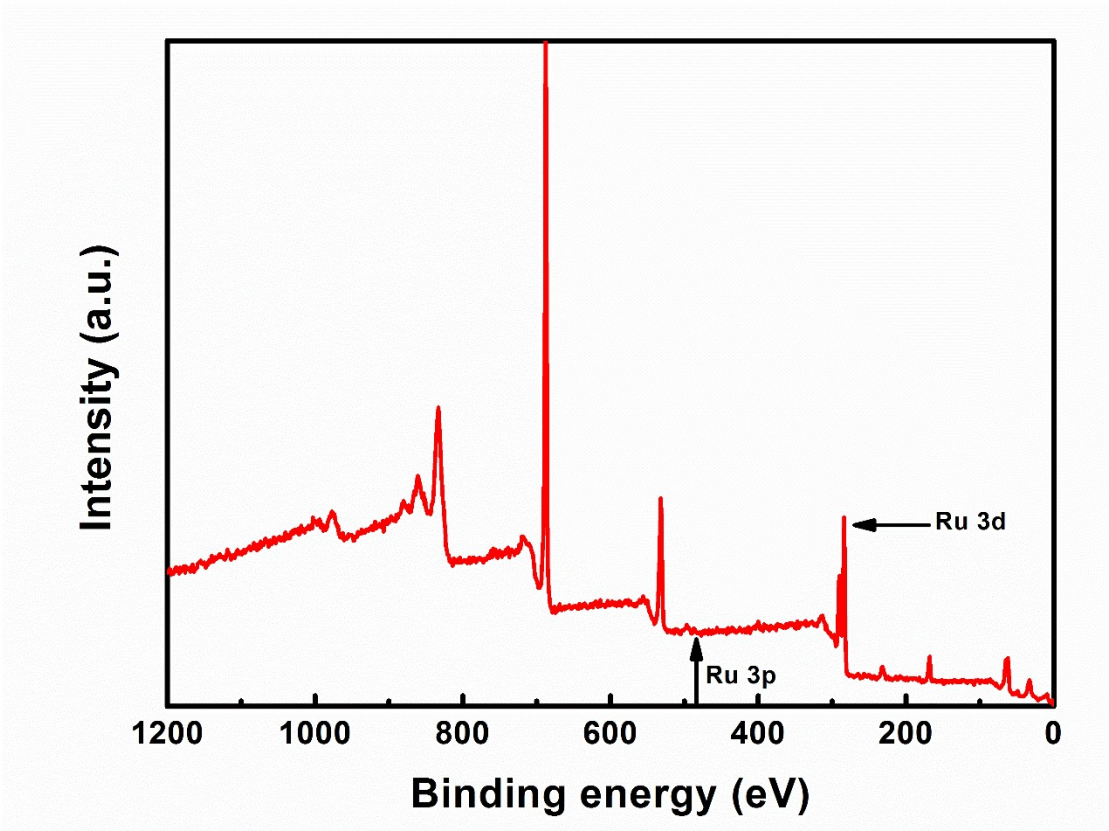

Fig. S16. XPS results after durable test.

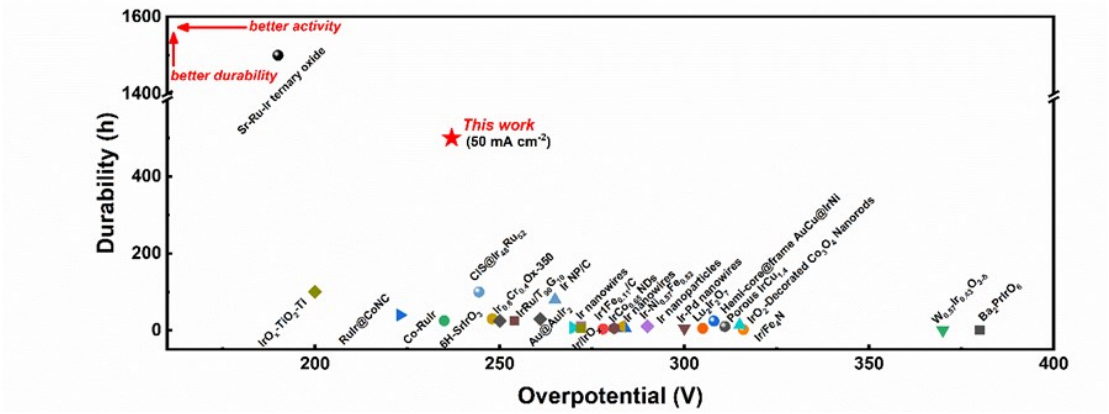

Fig. S17. Comparison of overpotentials and durability at 10 mA cm^{-2} for Ru-IrOx and other reported Ir-based acidic OER catalysts.

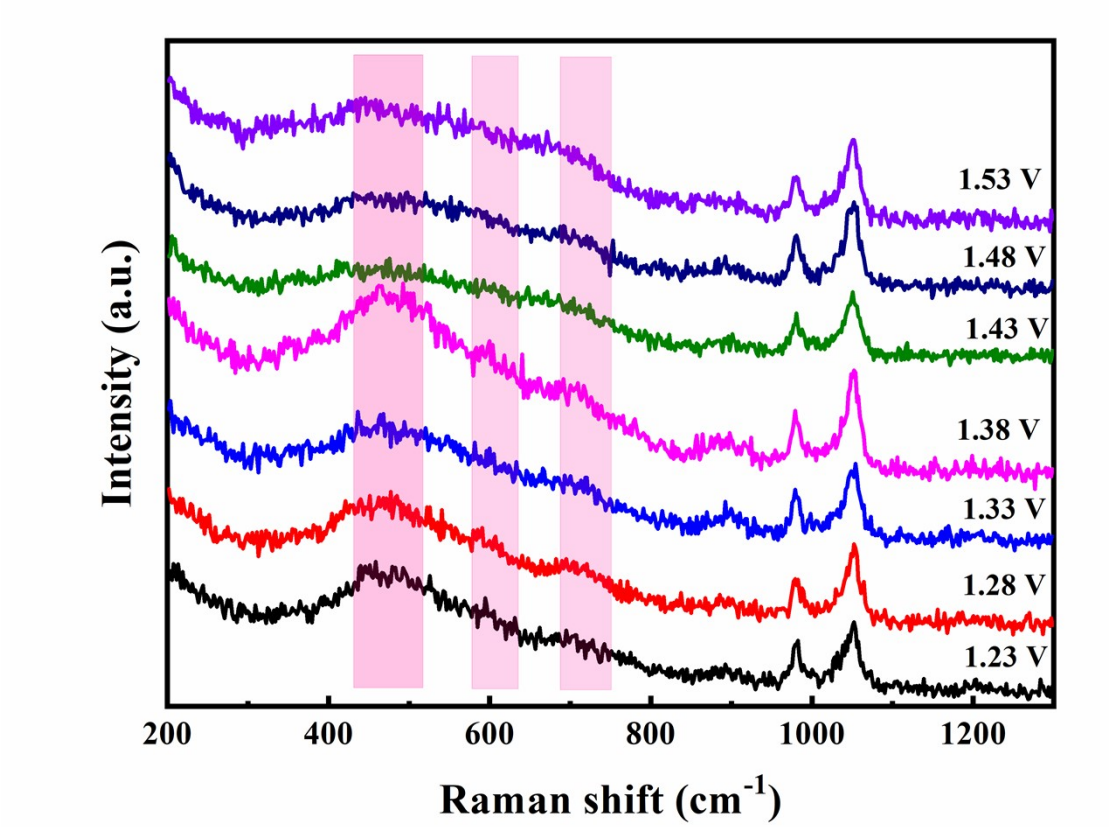

Fig. S18. In-situ Raman spectra of Ru-IrO_x in the potential range of 1.53-1.23 V vs. RHE.

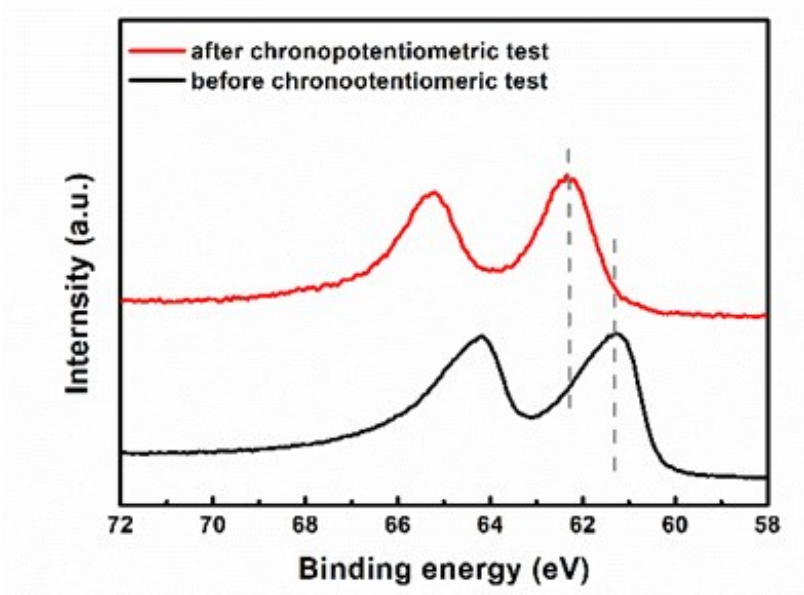

Fig. S19. High-resolution XPS results of Ir 4f for Ru-IrO_x before and after chronopotentiometric test.

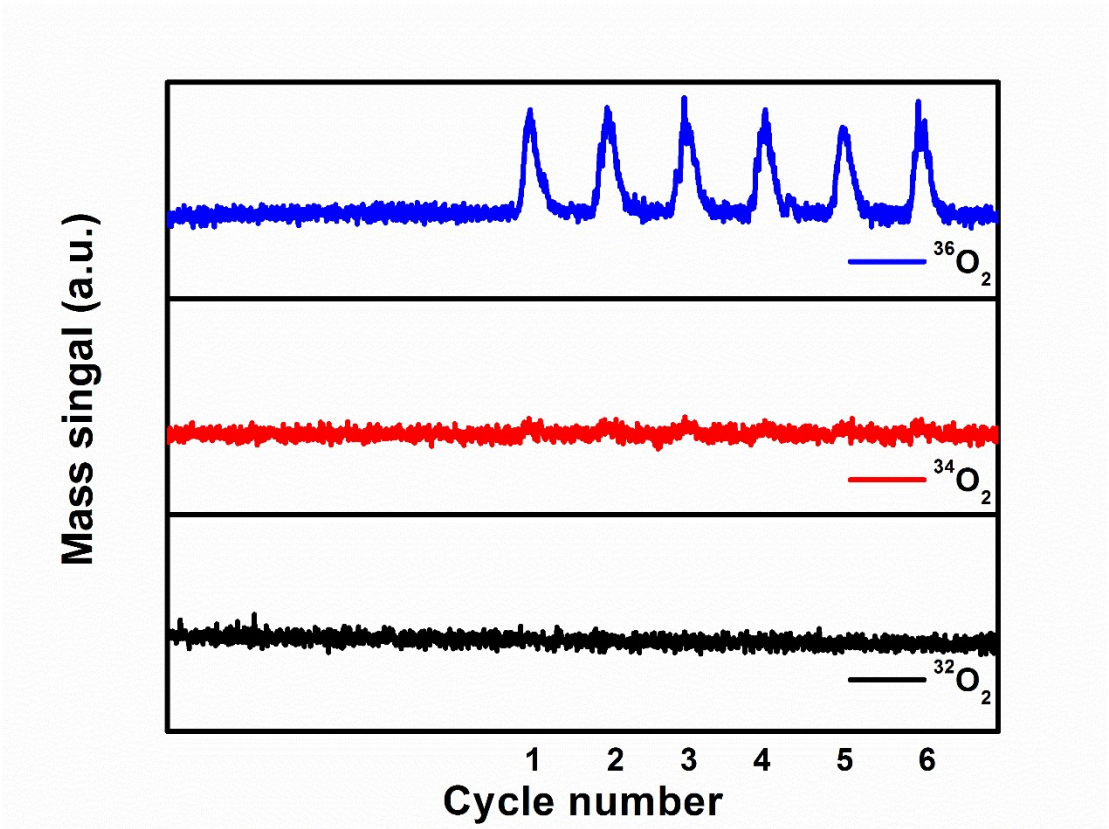

Fig. S20. DEMS signals of O_2 products for Ru-IrO_x clusters in the electrolyte using $H_2{}^{18}O$ as the solvent during six times of CVs in the potential range of 1.11-1.66 vs. RHE.

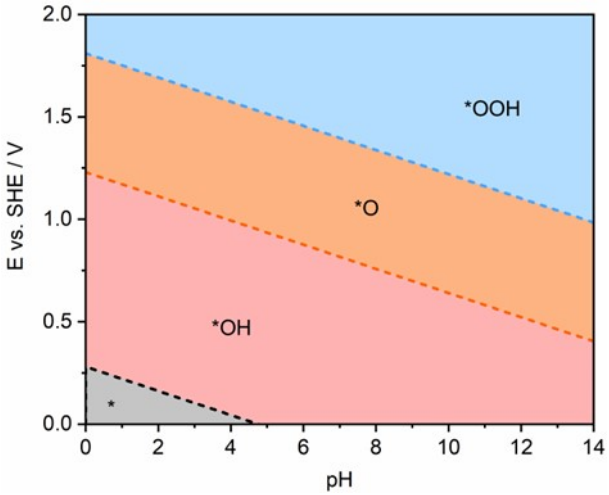

Fig. S21. The surface Pourbaix diagram of IrO_2(110) surface. The stable phases are highlighted by pink for *OH, orange for *O and blued for *OOH, respectively. labelled as on the pictures.

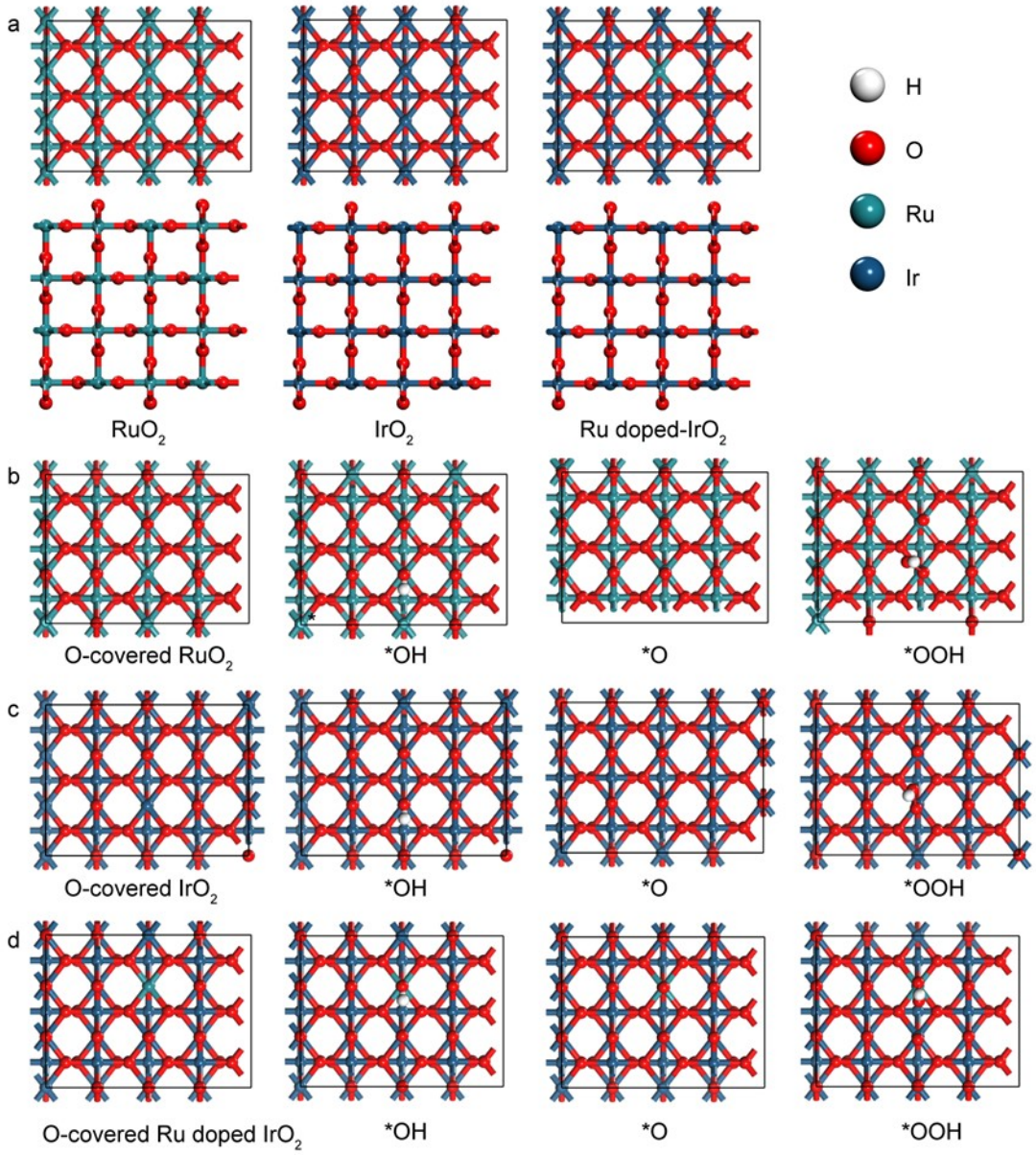

Fig. S22. (a) The top and side views of RuO_2(110), IrO_2(110) and Ru-doped IrO_2(110) models. (b-c) Structures of O-covered RuO_2(110), IrO_2(110) and Ru-doped IrO_2(110) and their *OH, *O and *OOH intermediates of OER process.

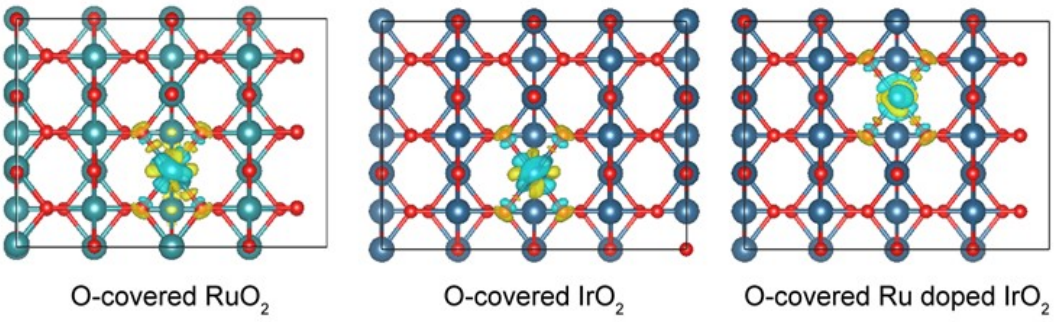

Fig. S23. The charge-density difference of O-covered RuO_2(110), IrO_2(110) and Ru-doped IrO_2(110). Yellow and cyan isosurfaces indicate the gain and loss of electrons. The isosurface level is set as 0.015 eVÅ^{-3}.

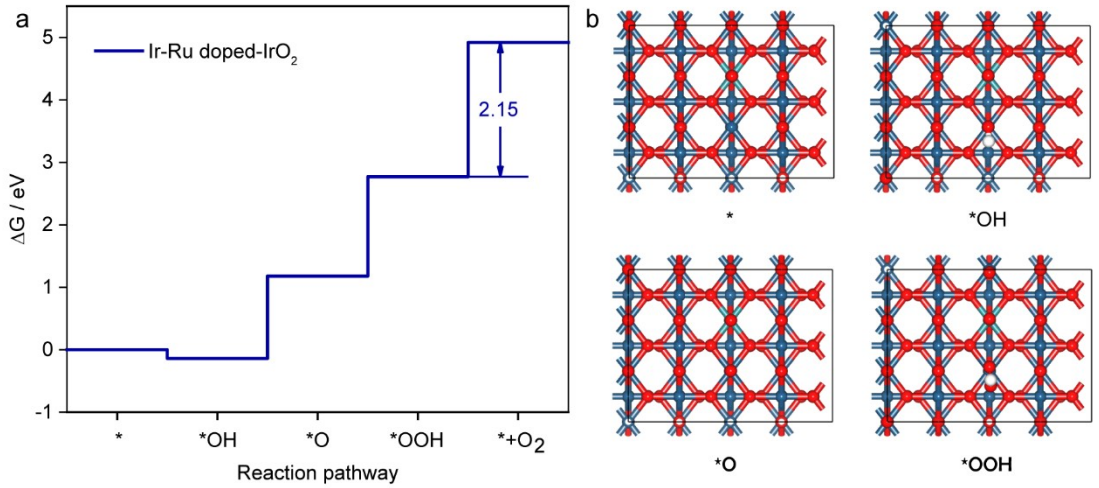

Fig. S24 (a) Gibbs free energy diagrams and (b) structures of intermediates for OER processes on Ir site of Ru-doped IrO_2(110), which are simplified as Ir-Ru-doped IrO_2 for clarity. Red, white and dark blue balls represent O, H and Ir atoms.

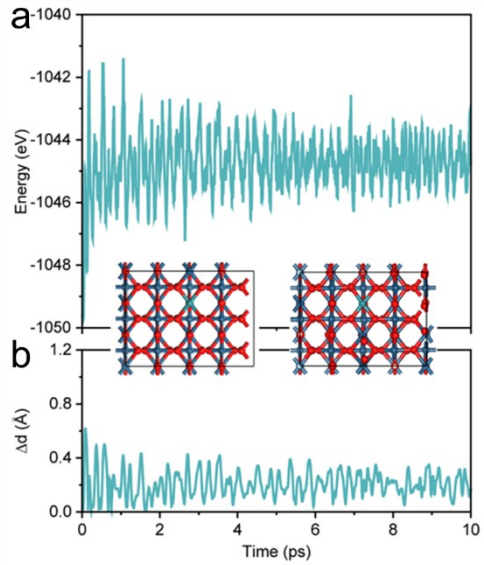

Fig. S25 The AIMD results of Ru doped IrO_2 at 500K for a total time of 10 ps and time step of 2fs under the canonical ensemble using Nosé thermostat. The total energy (a) and position changes (△d, Å) (b) of Ru atom relative to the initial Ru during AIMD. The inset pictures show the structures of Ru doped IrO_2 before and after AIMD.

Table S1. Textural parameters of Ru-IrO_x.

Sample	BET surface area	Micropore volume	Total pore volume
Ru-IrO_x	22.2 m^2 g^{-1}	0.002761 cm^3 g^{-1}	0.055 cm^3 g^{-1}

Table S2. Ru and Ir content in Ru-IrO_x clusters.

Sample	Ru (wt %)	Ir (wt %)
Ru-IrO_x	4.67	55.15

Table S3. Structural parameters of Ru and reference samples extracted from the Ru K-edge EXAFS fitting

Sample	**bond type**	**CN**	**R (Å)**	**σ^2 (10^{-3}Å^2)****	**R factor**
Ru-foil	Ru-Ru	12	2.67±0.01	2.4±0.5	0.015
RuO_2	Ru-O	5.7±1.7	1.96±0.01	2.4±1.1	0.012
Ru-IrO_x	Ru-O	3.0±1.3	2.11±0.01	8.2±1.5	0.005

*CN: coordination number; S_0^2 was fixed to be 0.67 from Ru-foil.

** σ^2: Debye−Waller factors

Table S4. Structural parameters of Ir and reference samples extracted from the Ir L_3-edge EXAFS fitting.

Sample	**bond type**	**CN***	**R (Å)**	**σ^2 (10^{-3}Å^2)****	**R factor**
Ir foil	Ir-Ir	12	2.71±0.01	2.9±0.4	0.001
IrO_2	Ir-O	6.2±0.4	2.02±0.01	4.3±0.6	0.009
Ru-IrO_x	Ir-O	4.3±0.5	2.04±0.01	4.1±1.3	0.014
Ir	Ir-O	2.7±0.5	2.02±0.02	6.9±0.2	0.017

*CN: coordination number; S_0^2 was fixed to be 0.70 from Ir-foil.

** σ^2: Debye−Waller factors

Reference

[1] G. Kresse, J. Furthmüller, *Phys. Rev. B* **1996**, 54, 11169.

[2] J. P. Perdew, K. Burke, M. Ernzerhof, *Phys. Rev. Let.* **1996**, 77, 3865.

[3] P. E. Blöchl, *Phys. Rev. B* **1994**, 50, 17953.

[4] S. Grimme, J. Antony, S. Ehrlich, H. Krieg, *J. Chem. Phys.* **2010**, 132, 154104.

[5] a) A. A. Peterson, F. Abild-Pedersen, F. Studt, J. Rossmeisl, J. K. Nørskov, *Energy Environ. Sci.* **2010**, 3, 1311; b) J. K. Nørskov, J. Rossmeisl, A. Logadottir, L. Lindqvist, J. R. Kitchin, T. Bligaard, H. Jónsson, *J. Phys. Chem. B* **2004**, 108, 17886.

[6] J. K. Nørskov, T. Bligaard, A. Logadottir, J. R. Kitchin, J. G. Chen, S. Pandelov, U. Stimming, *J. Electrochem. Soc.* **2005**, 152, J23.